Contract No:

This document was prepared in conjunction with work accomplished under Contract No. 89303321CEM000080 with the U.S. Department of Energy (DOE) Office of Environmental Management (EM).

Disclaimer:

Effect of Nitrogen Blanketing on Soil-Side Corrosion Mitigation of the Double Shell Tanks at Hanford

Pavan K. Shukla, Roderick E. Fuentes, and
Bruce J. Wiersma
Savannah River National Laboratory®
Aiken, South Carolina, 29808
USA

Crystal Girardot, Jason Page, and
Shawn Campbell
Washington River Protection Solutions
2425 Stevens Center Pl
Richland, Washington, 99352
USA

ABSTRACT

Radioactive waste is stored in underground, carbon-steel double-shell tanks at the Department of Energy Hanford site. The double-shell tank design includes a secondary shell surrounding the primary shell, where the bottom plate of the secondary shell rests on a concrete pad that contain drainage channels. There have been instances of metal loss on the secondary shell bottom plates in contact with the concrete foundation where groundwater accumulation in the channels may have caused corrosion. In addition, uneven contact between the foundation and shell could create occluded areas where localized corrosion is potentially more severe. In previous studies, vapor corrosion inhibitors (VCIs) were tested for their ability to mitigate concrete-foundation-side, i.e., concrete-side, corrosion of the secondary shell bottom. The previous studies showed that VCIs are effective in mitigating corrosion for both immersed and vapor space conditions. However, even distribution of the VCIs throughout the 85-ft diameter bottom of the secondary shell could be a challenge. This study investigated the feasibility of nitrogen blanketing to mitigate concrete-side corrosion of the secondary shell. Laboratory experiments were conducted to quantify the nitrogen blanketing effect on corrosion mitigation. The experimental data showed that nitrogen blanketing is as effective as VCIs in mitigating the concrete-side corrosion of the double shell tanks. Experimental results associated with the two corrosion mitigation methods for their application on the Hanford double-shell tanks are presented.

Key words: Nitrogen, Vapor Corrosion Inhibitors, Hanford, Double Shell Tanks, Bottom Plate, Pitting Corrosion.

INTRODUCTION

High-level radioactive waste generated during reprocessing of spent nuclear fuel at Hanford has been stored in 149 single- and 27 double shell tanks (DSTs). Each DST consists of a primary shell (inner) surrounded by secondary (outer) shell. The secondary shell's bottom rests on a concrete foundation. Rainwater leachate from the soil may seep in, and accumulate in the drain slots, and may corrode the exterior of the secondary liner. Several thinned-wall areas have been detected during ultrasonic inspections of the annulus floor between the primary and secondary tank shells. Since the inspection is confined to the annulus region, there is a concern that corrosion is widespread on the underside of bottom

plate. The rainwater leachate levels can vary in the drain slots as the LDPs are periodically pumped to remove water that has accumulated. Corrosion could be caused by direct contact with the accumulated water, and when the leak detection pit (LDP) water level is below the concrete foundation and the secondary shell bottom interface, vapor space corrosion (VSC) could also occur. The accumulated rainwater leachate is drained through the sumps in the LDP. The LDP water samples were analyzed for their constituents, and two simulants were developed considering the chemical composition range of the accumulated water. A version of the simulant identified as ground water (GW) was found to be most corrosive in a previous study.[1] The chemical composition of the GW simulant is listed in Table 1, and it has been used as a conservative representation of the rainwater leachate in several studies[2,3,4] where VCIs were evaluated for their effectiveness to mitigate the secondary liner bottom corrosion. Two other studies[5,6] also evaluated VCIs' performance for the soil-side corrosion of the aboveground storage tanks.

Uniform distribution of the VCIs throughout the 85-ft diameter bottom of the secondary shell could be a challenge because of the direct contact between the bottom plate and the slotted concrete foundation. The VCIs could preferentially accumulate in the slotted areas of the concrete foundation and may not reach in sufficient concentration to the bottom plate areas that are in direct contact with the foundation; this could result in accelerated corrosion in areas where VCIs migration is inhibited by the physical barrier of the concrete foundation. Considering the anticipated issues with the VCIs' distribution, the option of using nitrogen to de-aerate the liquid and the vapor space to mitigate corrosion of the steel. Nitrogen displaces oxygen, a key cathodic reactant for corrosion, in the liquid and vapor space and because it is inert with respect to the steel, the corrosion rate decreases significantly.[7]

Table 1
Composition of the Ground Water Simulant

Source chemical	Concentration (M)
Sodium bicarbonate	1.75×10^{-3}
Calcium hydroxide	1.50×10^{-3}
Potassium nitrate	2.40×10^{-4}
Strontium Nitrate	2.87×10^{-6}
Ferric sulfate	6.25×10^{-4}
Sodium Metasilicate, 5hydrate	6.00×10^{-4}
Ferric chloride	7.67×10^{-5}
Manganese Chloride	3.1×10^{-4}
Acetic Acid	3.0×10^{-4}
Adjusted pH	7.6

EXPERIMENTAL

Laboratory experiments were conducted to quantify the nitrogen blanketing effect on corrosion mitigation. An experiment was set up using GW simulant as the electrolyte. Disk coupons, machined from a legacy carbon steel plate, were used in the experiments. The legacy carbon steel is based on specifications of Association of American Railroads[(1)] Tank Car (AAR TC 128) steel, and its chemistry and microstructure are similar to the vintage steel from which the tanks were fabricated UNS K02401 (i.e., American Society for Testing and Materials (ASTM)[(2)] A515 Grade 60 carbon steel). The chemical composition of the legacy carbon steel is listed in Table 2. All elemental compositions except for Mn and Si meet the ASTM A515 Grade 60 specification. The coupons were 25 mm (1 inch) diameter with a thickness of approximately 3 mm (0.125 inch) and polished to a 600-grit finish. The coupons were potted in a mold prepared with a two-part transparent epoxy, such that that one face of the coupon was exposed to the

[(1)] American Association of Railroads, 425 3rd Street SW, Washington, DC 20024
[(2)] ASTM International, 100 Barr Harbor Dr., West Conshohocken, PA 19428-2959

test environment. The coupons' exposed surfaces were modified to simulate crevice corrosion. A crevice former was attached to each coupon surface using tape and wire. A crevice former was secured to each coupon surface using tape and wire (see configuration in Figure 1). The crevice former assembly partially covered the coupon surface, which created conditions for crevice corrosion. Note that the assembly does not ensure uniform tightness of the crevice for each sample.

Table 2
Chemical Composition of AAR TC 128 Steel (wt.%)

	C	Mn	P	S	Si	Fe
Specification	0.24 (max.)	0.9 (max.)	0.035 (max.)	0.04 (max.)	0.13 to 0.33	Balance
Measured	0.212	1.029	0.012	0.013	0.061	Balance

(a) Top view **(b) Side View**

Figure 1. (a) Top, and (b) Side views of the partially covered coupon. The coupon's surface is partially covered with a crevice former, which is held in place using purple wire and tape.

A glass vessel of dimensions 1.0 m (3.3 ft) tall and 14 cm (5.5 inch) diameter was used for the experiment. Approximately 1.25 L of GW simulant was added to a vessel for the experiment. The vessel has a water jacket around the simulant holding area. The simulant was maintained at a constant temperature by circulating water at 45 ± 2 °C through the jacket. This temperature mimics the maximum temperature of the liquid in the LDP system. The temperature of the vapor space was not controlled or monitored. The vessel also has several ports, which were used to insert a thermocouple, three electrical resistance (ER) probes, and one dissolved-oxygen sensor. An image of the experimental system is presented Figure 2. Coupons were exposed to the electrolyte and vapors of the electrolyte in the experiment by suspending them using a rod. The coupons were suspended such that the exposed surfaces of the vapor space coupons were facing the electrolyte. The vapor space coupons were placed at several height levels with respect to the electrolyte using the rod. The coupons' positions, with respect to electrolyte in the vessel, simulated different vapor space conditions and water levels in the drain slots, i.e., drainage channels. These levels, representing the drain slot characteristics and its position with respect to the bottom, are described:

Level 1: Bottom or low level. Coupons were dipped in the simulant for five minutes prior to testing. The coupons were hung at the bottom fixed ring of the rod. These coupons were suspended approximately 25 mm (1 inch) above the liquid level of the simulant. Every two weeks, the coupons were lowered into the simulant for 5 minutes when the coupons were in GW only, but the coupons were not lowered into the simulant during the nitrogen addition. This level is representative of the situation when the bottom plate experienced periodic wetting and drying.

Level 2: Intermediate or middle level. Coupons were dipped in the simulant for five minutes prior to testing. The coupons were hung at the middle-fixed ring approximately 46 cm (18 inch) above the liquid simulant in each vessel. This level is representative of a vapor space region of the secondary liner bottom that was once exposed to water but currently has infrequent or no contact with the water. However, this region is exposed to the humidified air.

Level 3: Top or high level. This set of coupons was not exposed to the solution prior to testing. The coupons were suspended approximately 92 cm (36 inch) above the simulant. This level is representative of the secondary liner bottom plate region that is only exposed to the humidified air and any volatile species from the solution.

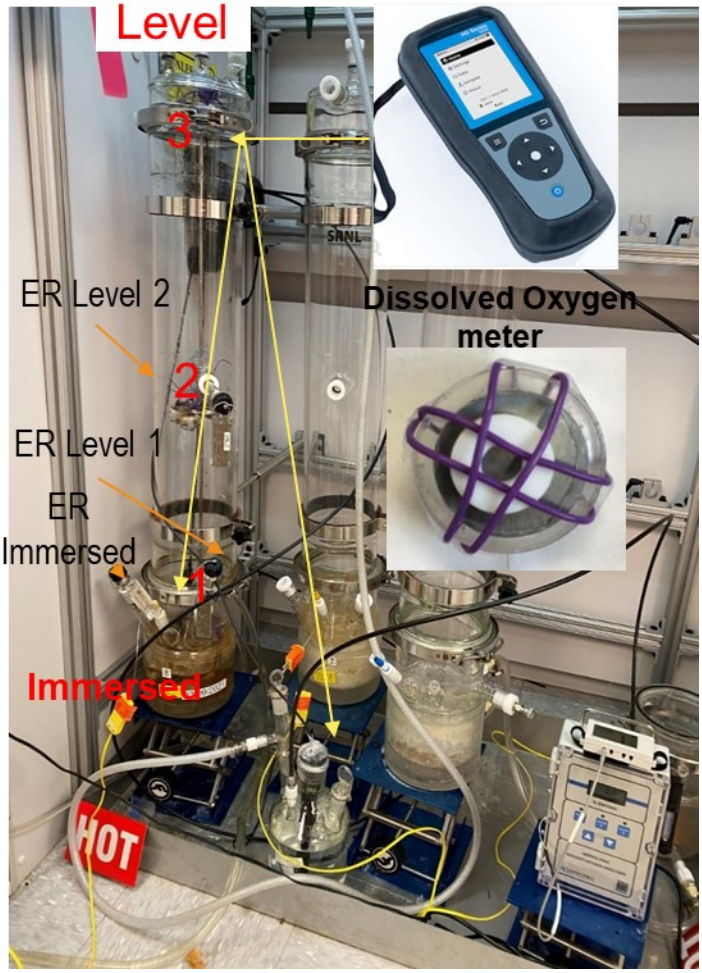

Figure 2. Image of the experimental setup.

Initially, the coupons at each level were exposed to the GW simulant only for 78 days, without any nitrogen. The GW simulant was then purged with nitrogen starting on the 78th day of the experiment; the purging continued for the next 120 days. In addition, simultaneous to the start of nitrogen purging, another set of coupons at each level were loaded in the experimental vessel; three coupons each at Levels 1, 2, and 3, and four coupons immersed in GW. Furthermore, when nitrogen was added to the vessel, a port on the top lid of the vessel was fitted with a tube that passed through a water trap; this allowed flow of the nitrogen through the vessel. The dissolved oxygen concentrations were measured in the GW simulant and water trap. In addition, the oxygen concentration was also measured in the outflow gas that passed through the water trap.

The dissolved oxygen (DO) concentration data just before adding nitrogen and after the addition in the experimental vessel and in water trap are presented in Figure 3(a). The DO values are close to 9 ppm before the addition, and close to zero after the addition. The time lag between the start of the nitrogen addition and DO values reaching zero was negligible. As seen in Figure 3(a), the GW simulant temperature remained close to 45 °C throughout the experimental duration. The gas phase oxygen

concentration data is presented in Figure 3(b); as seen in the figure, the gas phase oxygen concentration quickly reached zero after addition of nitrogen.

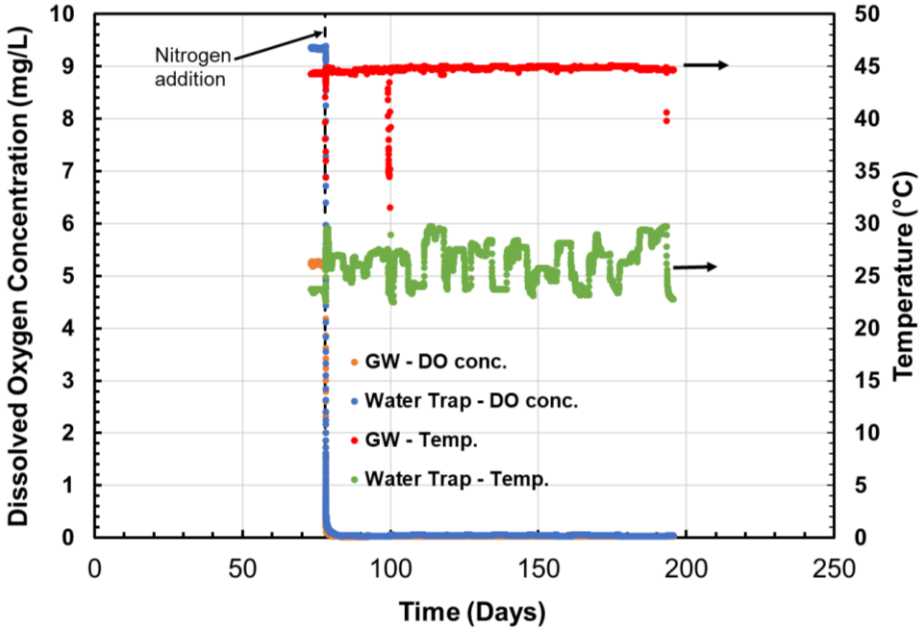

(a) Dissolved oxygen and temperature versus time

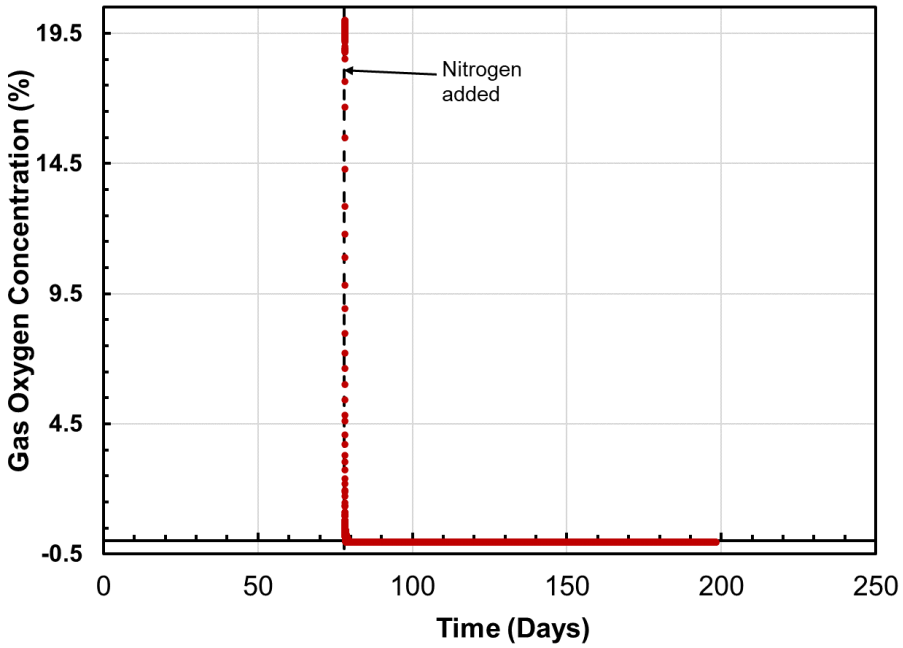

(b) Gas phase oxygen concentration versus time

Figure 3. (a) Dissolved oxygen concentration and temperature and (b) gas phase oxygen concentration versus time.

Coupons were acid cleaned using the Clark solution,[8] and each coupon's mass change was also recorded. In addition, coupon surfaces were profiled and the deepest pit in each coupon was measured using the surface profile data. The coupons' surfaces were profiled using a visible light profilometer.

EXPERIMENTAL DATA AND RESULTS

Post-test images of the coupons are presented in Figure 4. Pitting and patch-like corrosion occurred on all the coupons. Images of the coupons sequentially exposed to GW only for 78 days and GW + N_2 for 120 days are presented in Figure 4(a), and images of the coupons exposed to GW + N_2 for 120 days are presented in Figure 4(b). As seen in the figures, the coupons sequentially exposed to GW only and GW + N_2 electrolytes accumulated significantly more corrosion products compared to the coupons that were exposed the GW + N_2 electrolyte.

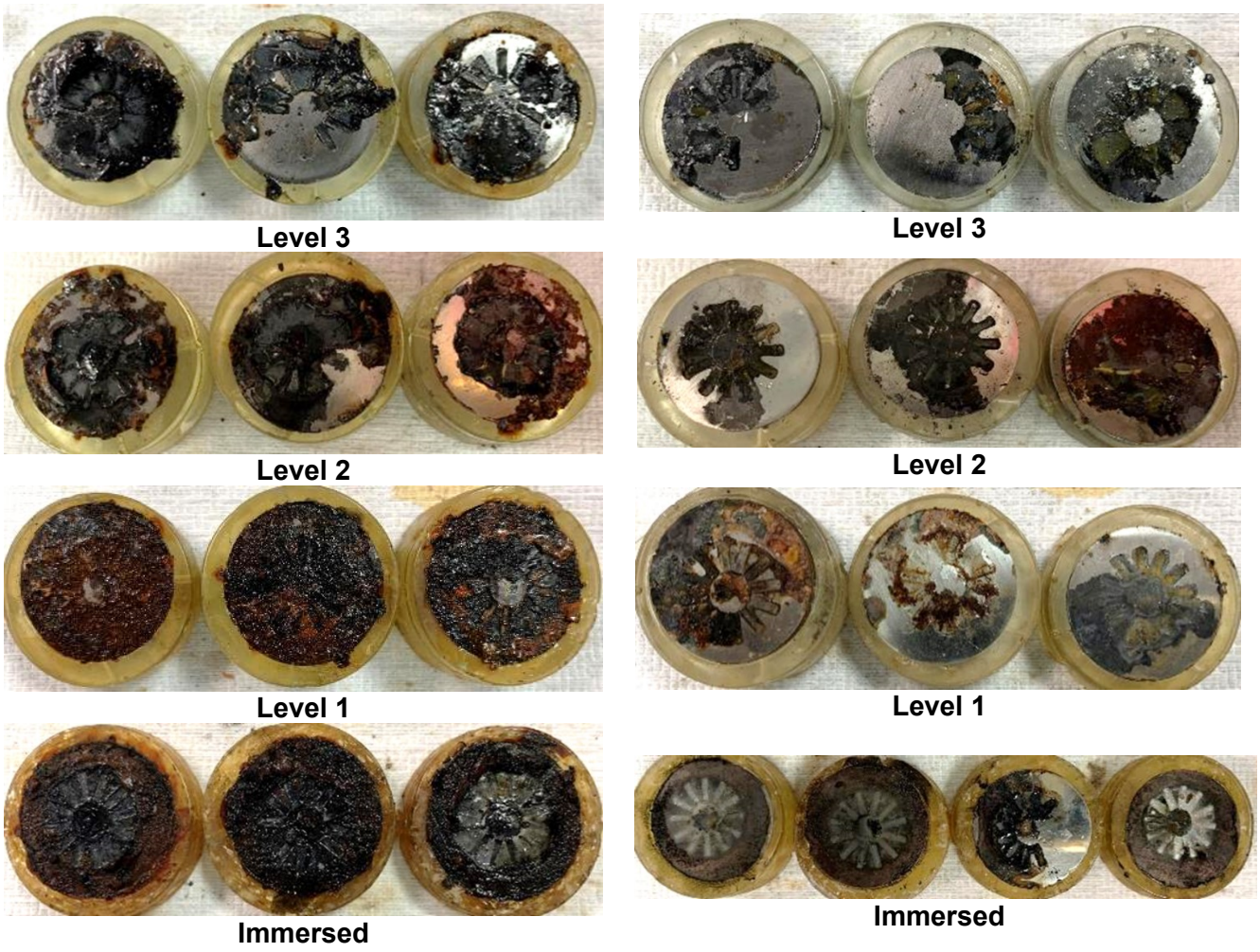

(a) Exposed to GW only for 78 days and GW + N_2 for 120 days

(b) Exposed to GW + N_2 for 120 days

Figure 4. Images of the coupons exposed to (a) GW only for 78 days and GW +N_2 for 120 days, and (b) GW + N_2 for 120 days.

The ER probe data were collected using the cylindrical probe elements located at Levels 1 and 2 and immersed in the solution. The probes' data and the derived corrosion rates are presented in Figure 5; for the immersed probe in Figure 5(a), and for Levels 1 and 2 in Figure 5(b) and Figure 5(c), respectively. As seen in the figures, the corrosion rates reduced significantly after the nitrogen purge start.

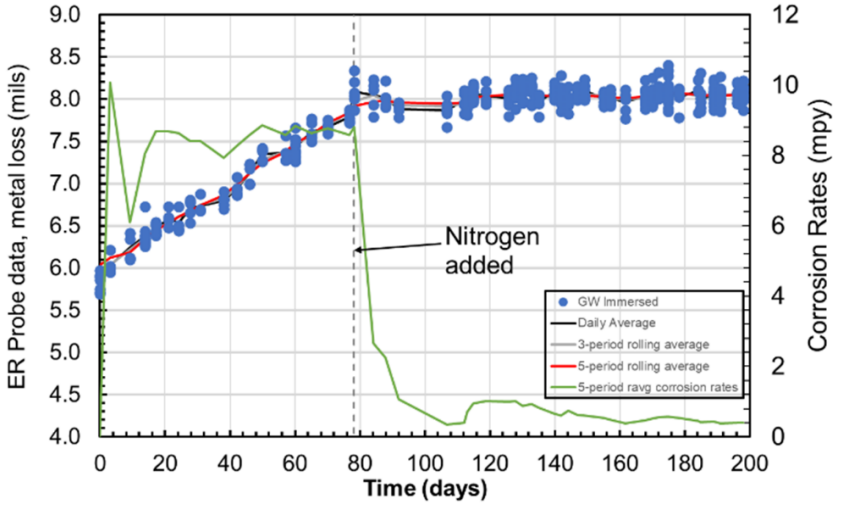

(a) Immersed

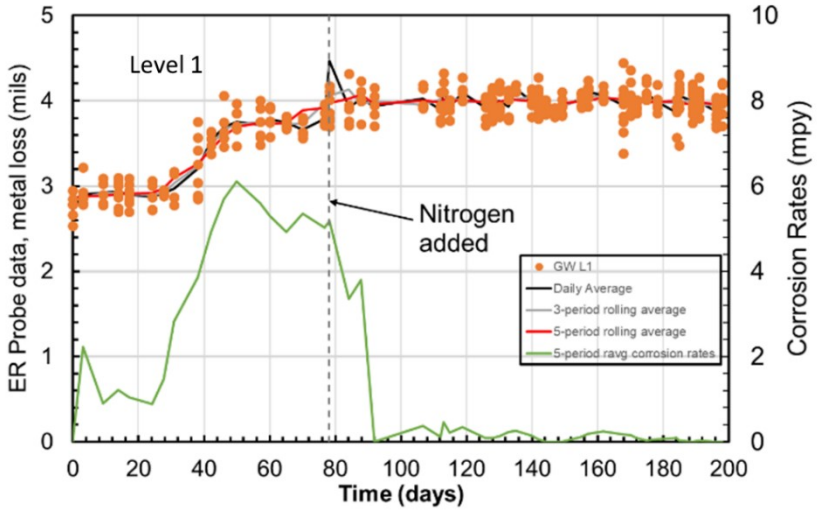

(b) Level 1

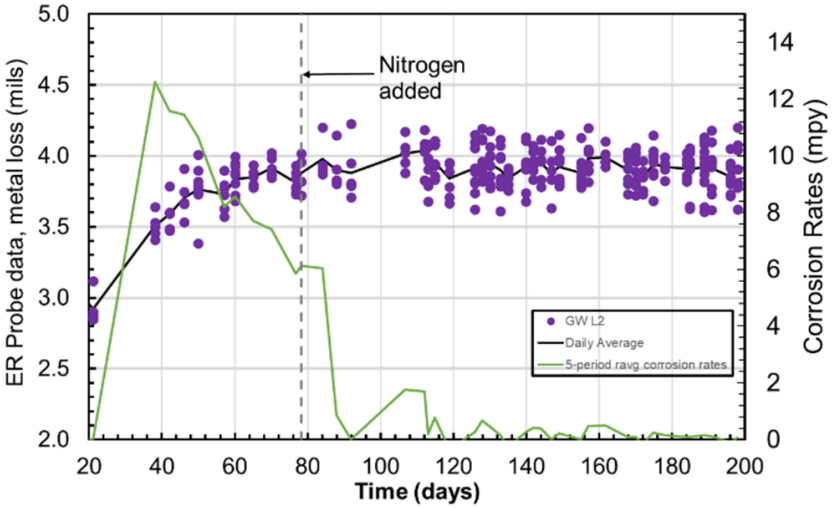

(c) Level 2

Figure 5. Electrical resistance data and corresponding corrosion rates for the probes located in (a) immersed, (b) Level 1, and (c) Level 2.

The corrosion rate data of the coupons sequentially exposed to GW and GW + N_2 electrolytes are listed in Table 3, and the corrosion rate data of the coupons exposed to GW + N_2 electrolyte are listed in Table 4. The average of the surface average and deepest pit corrosion rates for the GW and GW + N_2 electrolytes coupons is graphically presented in Figure 6. Similarly, the averages of the surface average and deepest pit corrosion rates for the GW + N_2 electrolyte coupons are graphically presented in Figure 7. The surface average corrosion rates are an order of magnitude lower in GW + N_2 compared to GW and GW + N_2, and the deepest pit corrosion rates are approximately lower by a factor of three in GW + N_2 compared to GW and GW + N_2. The corrosion rate data in Figure 6 and Figure 7 clearly show that the corrosion rates are significantly reduced in presence of nitrogen, and nitrogen purging could be an effective corrosion mitigation strategy.

Table 3
Corrosion Rates of the Coupons Exposed to GW for 78 days and GW+N_2 for 120 days

Level	Corrosion Type	Corrosion Rate (mpy)			Average + Std of Surface Average Corrosion Rate (mpy)	Average + Std of Deepest Pit Corrosion Rate (mpy)
		Coupon 1	Coupon 2	Coupon 3		
Level 3	Surface Average	1.23	0.99	0.83	1.02 ± 0.20	12.1 ± 5.1
	Deepest Pit Corrosion	9.2	18.1	9.1		
Level 2	Surface Average	1.72	1.49	1.90	1.70 ± 0.20	15.0 ± 3.3
	Deepest Pit Corrosion	18.4	11.8	14.7		
Level 1	Surface Average	1.27	1.64	1.78	1.27 ± 0.26	15.3 ± 6.5
	Deepest Pit Corrosion	22.5	13.3	10.0		
Immersed	Surface Average	2.75	2.46	3.37	2.86 ± 0.46	15.6 ± 3.3
	Deepest Pit Corrosion	12.7	14.7	19.2		

Table 4
Corrosion Rates of the Coupons Exposed to GW+N_2 for 120 days

Level	Corrosion Type	Corrosion Rate (mpy)				Average + Std of Surface Average Corrosion Rate (mpy)	Average + Std of Deepest Pit Corrosion Rate (mpy)
		Coupon 1	Coupon 2	Coupon 3	Coupon 4		
Level 3	Surface Average	0.30	0.60	0.45	–	0.45 ± 0.15	5.9 ± 0.9
	Deepest Pit Corrosion	4.9	6.2	6.7	–		
Level 2	Surface Average	0.38	0.26	0.42	–	0.35 ± 0.08	5.6 ± 0.6
	Deepest Pit Corrosion	6.0	5.6	5.0	–		
Level 1	Surface Average	0.37	0.17	0.42	–	0.32 ± 0.13	6.7 ± 2.0
	Deepest Pit Corrosion	7.7	8.1	4.4	–		
Immersed	Surface Average	0.32	0.27	0.34	0.42	0.33 ± 0.06	3.7 ± 1.5
	Deepest Pit Corrosion	2.3	2.6	4.9	5.1		

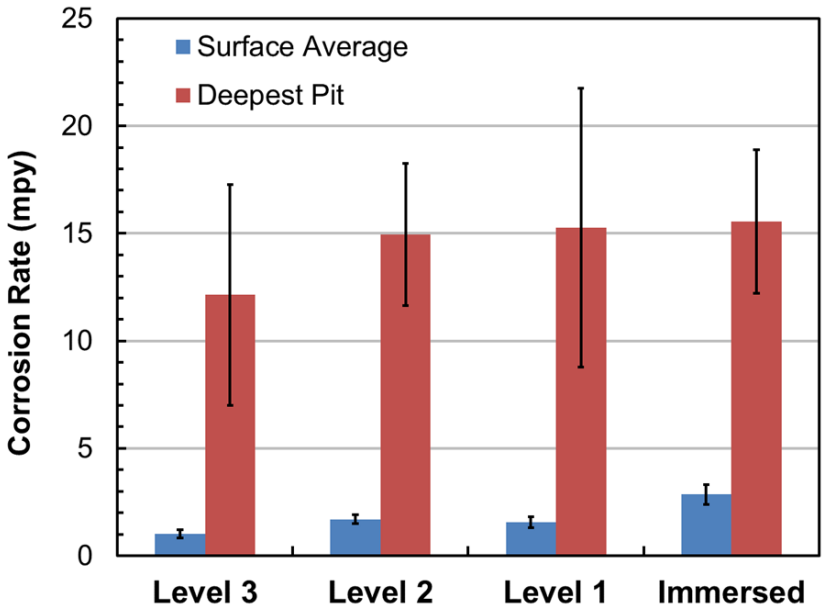

Figure 6. Surface average and deepest pit corrosion rates of the coupons sequentially exposed to GW for 78 days and GW + N_2 for 120 days. The standard deviations of the corrosion rates are represented by a solid black line in each bar.

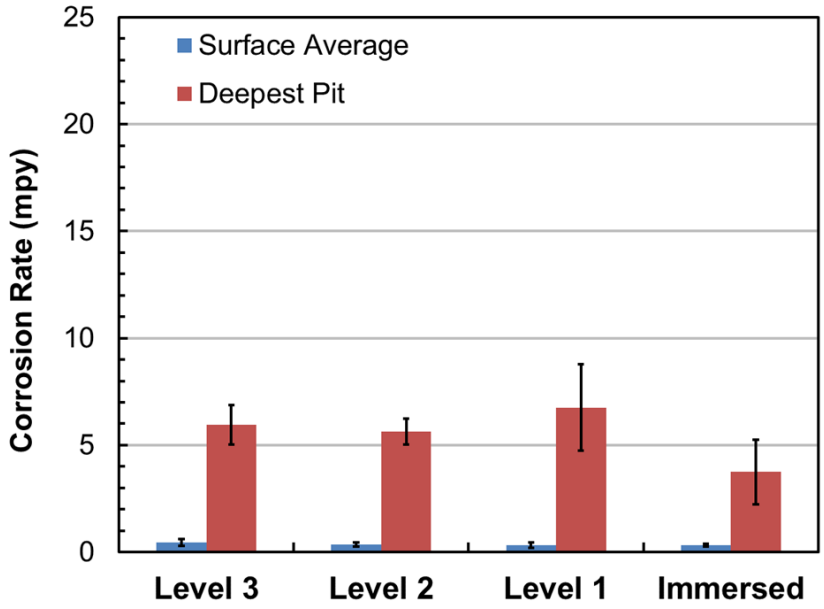

Figure 7. Surface average and deepest pit corrosion rates of the coupons exposed to GW + N_2 for 120 days. The standard deviations of the corrosion rates are represented by a solid black line in each bar.

The profiled images of the coupons exposed to GW and GW + N_2 are presented in Figure 8. Similarly, profiled images of the coupons exposed to GW + N_2 are presented in Figure 9.

A comparison of the profiled images in Figure 8 and Figure 9 clearly shows that the coupons exposed to GW + N_2 corroded far less compared to the coupons exposed to GW and GW + N_2. The deepest pit corrosion rates of the coupons exposed to the GW + N_2 ranged between 3 to 6 mpy. The pit depths on the GW + N_2 coupons ranged between 19 to 68 µm; the deepest pit depth on the majority of the coupons ranged between 35 to 55 µm; these smaller-depth pits could have formed when the coupons were initially placed in the vessel as the initial corrosion rates are generally higher than the long-term corrosion rates on carbon steel.

The corrosion rates of the coupons exposed to GW + N_2 are compared with the corrosion rates of the coupons that were exposed to GW + 100% VCI-B; the 100% VCI-B data published in Shukla et al.[4] The tests with the vapor corrosion inhibitor (VCI) were performed in the same equipment, conditions and with the same type of samples as the tests that were performed with nitrogen. The comparison is shown in Table 5. The averages of the surface average corrosion rates for the coupons in immersed and Level 1 are less than 0.5 mpy for both the exposure conditions. Similarly, the deepest pit corrosion rates of the coupons exposed to the two electrolytes conditions are similar. This comparison is not completely accurate as the exposure times are different for the two environments. That it is, it is unknown as to whether an additional 60 days of exposure to nitrogen will demonstrate whether it is better, the same or worse than the VCI. A complete comparison could be made by performing the tests with nitrogen for 180 days. Nevertheless, the results do indicate that both nitrogen and the VCI are effective corrosion inhibitors, for their given exposure times, if they are maintained at effective concentration levels.

The corrosion rates of the coupons exposed to GW and GW + N_2 are compared with the corrosion rates of the coupons that were exposed to GW and GW + 100% VCI-B, and GW and GW + 50% VCI-B; the 100% and 50% VCI-B data were published in Shukla et al.[3] The averages of the surface average corrosion rates at a given level for the three exposure conditions overlapped, showing that the coupons underwent a similar level of corrosion under the three exposure conditions. Similarly, the deepest pit corrosion rates at Levels 1 through 3 overlap with each other. The deepest pit corrosion rates of the

coupons immersed in GW and GW + N_2 and in GW and GW + 50% VCI-B also overlap. This comparison further highlights that the corrosion mitigation performance of nitrogen is comparable to the effective concentrations of the VCI-B.

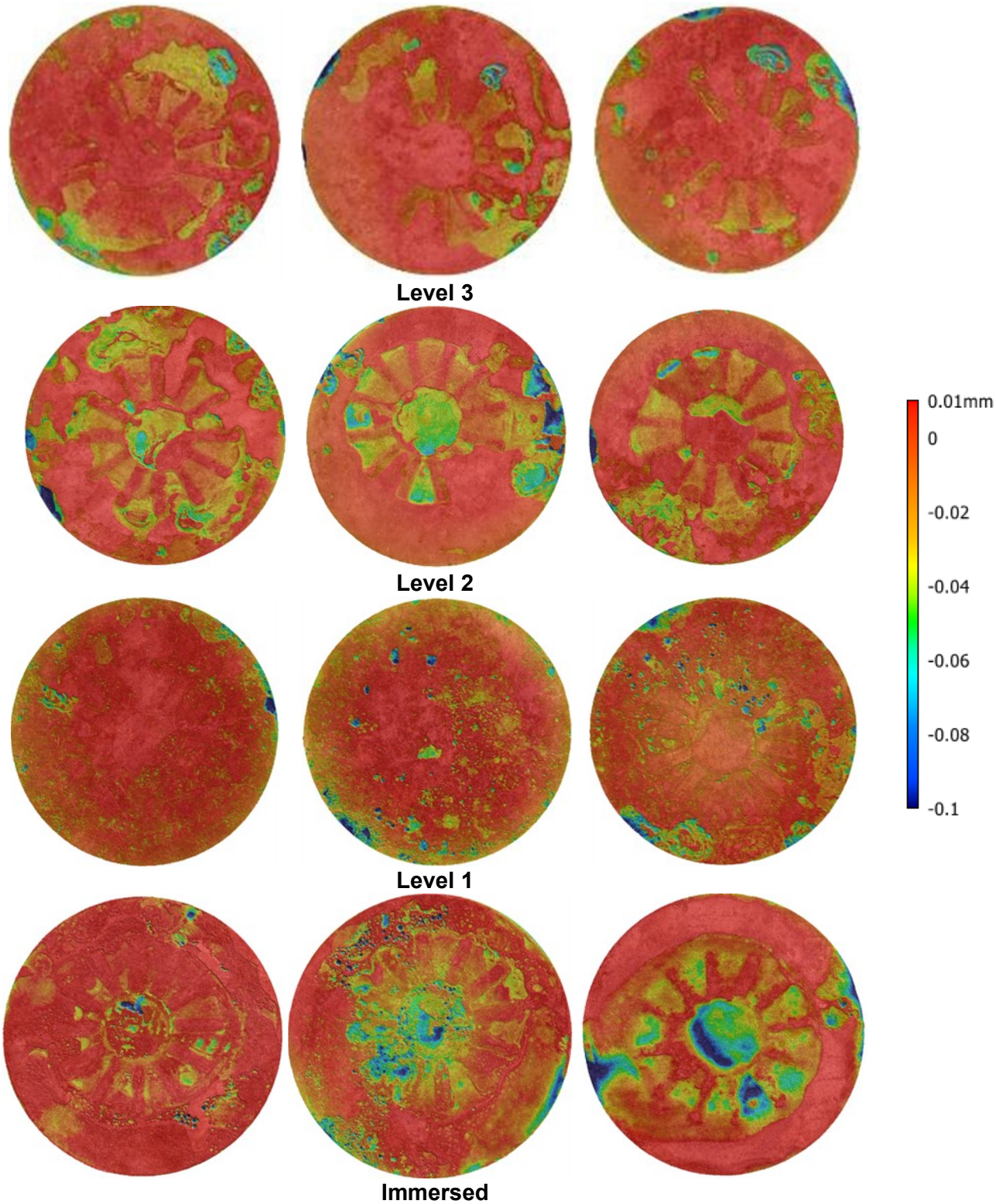

Figure 8. Profiled images of the coupons sequentially exposed to GW for 78 days and GW +N_2 for 120 days.

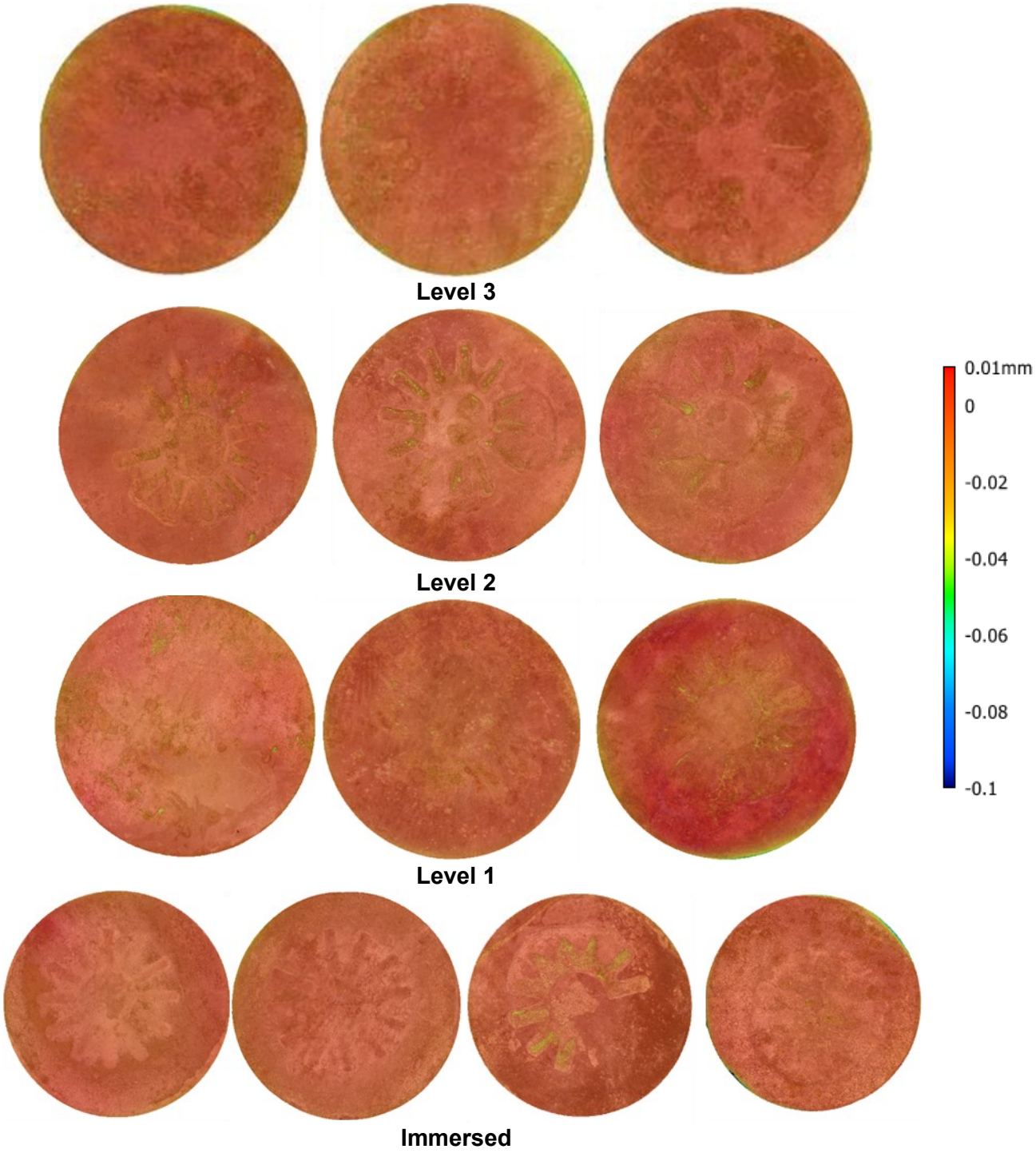

Figure 9. Profiled images of the coupons sequentially exposed to GW +N_2 for 120 days.

Table 5
Corrosion Rates of the Coupons Exposed to GW+N_2 for 120 days and to GW + 100% VCI-B for 180 days

Level	Coupons Exposed to GW + N_2 for 120 days		Coupons Exposed to GW + 100% VCI-B for 180 days	
	Surface Average Corrosion Rate + Standard Deviation (mpy)	Deepest Pit Corrosion Rate + Standard Deviation (mpy)	Surface Average Corrosion Rate + Standard Deviation (mpy)	Deepest Pit Corrosion Rate + Standard Deviation (mpy)
Level 1	0.32 ± 0.13	6.7 ± 2.0	0.34 ± 0.34	8.0 ± 0.7
Immersed	0.33 ± 0.06	3.7 ± 1.5	0.17 ± 0.03	1.2 ± 0.2

Table 6
Corrosion Rates of the Coupons Sequentially Exposed to GW for 78 days and GW+N_2 for 120 days,
GW for 60 days and GW + 100% VCI-B for 120 days, and GW for 60 days and GW + 50% VCI-B for 120 days.

Level	Coupons Exposed to GW and GW + N_2		Coupons Exposed to GW and GW + 100% VCI-B		Coupons Exposed to GW and GW + 50% VCI-B	
	Surface Average Corrosion Rate + Standard Deviation (mpy)	Deepest Pit Corrosion Rate + Standard Deviation (mpy)	Surface Average Corrosion Rate + Standard Deviation (mpy)	Deepest Pit Corrosion Rate + Standard Deviation (mpy)	Surface Average Corrosion Rate + Standard Deviation (mpy)	Deepest Pit Corrosion Rate + Standard Deviation (mpy)
Level 3	1.0 ± 0.2	12.1 ± 5.1	1.4 ± 0.1	13 ± 5.0	1.8 ± 1.4	10.5 ± 1.2
Level 2	1.7 ± 0.2	15.0 ± 3.3	1.9 ± 0.3	14 ± 3.0	1.7 ± 1.0	8.5 ± 0.6
Level 1	1.3 ± 0.3	15.3 ± 6.5	1.6 ± 0.3	11 ± 2.5	1.0 ± 0.1	14 ± 1.5
Immersed	2.9 ± 0.5	15.6 ± 3.3	3.1 ± 0.2	6.3 ±0.4	2.0 ± 0.2	20 ± 8

SUMMARY

The effectiveness of a nitrogen blanket for mitigating corrosion of the Hanford DSTs was investigated. The laboratory testing data showed the surface average corrosion rates are reduced by an order of magnitude in the presence of nitrogen when compared with the uninhibited conditions. These test results were compared with similar tests that were performed with a VCI. Although a complete comparison could not be made at this time due to differences in the exposure time the results seem to suggest that both effectively mitigate corrosion. A more complete comparison could be made by performing the nitrogen test for 180 days. In addition, the nitrogen and VCI-B comparison also showed that similar level of corrosion inhibition is achieved when weathered coupons were exposed to nitrogen, 100% VCI-B and 50% VCI-B.

ACKNOWLEDGEMENT

This work was produced by Battelle Savannah River Alliance, LLC under Contract No. 89303321CEM000080 with the U.S. Department of Energy. Publisher acknowledges the U.S. Government license to provide public access under the DOE Public Access Plan (http://energy.gov/downloads/doe-public-access-plan)."

REFERENCES

1. R. E. Fuentes, P. K. Shukla, B. J. Wiersma, C. Girardot, N. Young and T. Venetz, "Effects of Vapor Corrosion Inhibitors on Corrosion of Secondary Liner in Double Shell Tanks at Hanford," CORROSION/2019, Paper No. C2019-13369 (Houston, TX, NACE, 2019).

2. P. Shukla, R. E. Fuentes, B. J. Wiersma, C. Girardot, N. Young, and T. Venetz, "Performance of Vapor Corrosion Inhibitors on Mitigating Corrosion of Secondary Liner in Double Shell Storage Tanks at Hanford," CORROSION/2020, Paper No. C2020-14846 (Houston, TX, NACE, 2020).

3. P. Shukla, R. E. Fuentes, B. J. Wiersma, C. Girardot, J. Page, "Performance of Vapor Corrosion Inhibitors for Localized Corrosion Mitigation of Double Shell Storage Tanks at Hanford," CORROSION/2021, Paper No. C2021-16629 (Houston, TX, NACE, 2021).

4. P. K. Shukla, R. E. Fuentes, B. J. Wiersma, C. Girardot, J. Page, and S. Campbell, "Determining Migration of Vapor Corrosion Inhibitors Using Corrosion Potential Data," In Conference Proceedings of AMPP Annual Conference 2022, Paper no. C2022-17970, (Houston, TX, AMPP, 2022).

5. P. Shukla, X. He, O. Pensado, A. Nordquist, "Vapor Corrosion Inhibitors Effectiveness for Tank Bottom Plate Corrosion Control," Report Catalog Number PR–015–153602-R01 (Chantilly, VA: PRCI, Inc. 2018).

6. P. Shukla, A. Nordquist, R. Fuentes, B. Wiersma, L. Perry, "Determining Migration of Vapor Corrosion Inhibitions Through Sandpad," Report Catalog Number PR644-183611-R01. (Chantilly, VA: PRCI, Inc. 2022).

7. E. Schaschl and G. A. Marsh, "The Effect of Dissolved Oxygen on Corrosion of Steel and Current Required for Cathodic Protection," Corrosion, Vol. 35, No. 13, pp. 243-251, 1957.

8. ASTM International. ASTM G1–03 (Reapproved 2017), "Standard Practice for Preparing, Cleaning, and Evaluating Corrosion Test Specimens." West Conshohocken, Pennsylvania: ASTM International. 2014.